Special Issue: Vesuvius monitoring and knowledge

Somma Vesuvius volcano: ground deformations from CGPS observations (2001-2012)

Umberto Tammaro*, Prospero De Martino, Francesco Obrizzo, Giuseppe Brandi, Andrea D'Alessandro, Mario Dolce, Santa Malaspina, Claudio Serio, Folco Pingue

Istituto Nazionale di Geofisica e Vulcanologia, Sezione di Napoli, Osservatorio Vesuviano, Naples, Italy

Article history
Received November 2012; accepted June 2013.
Subject classification:
Ground deformation, CGPS, Somma-Vesuvius.

ABSTRACT

This paper is a contribution to the evaluation of ground deformations at Somma-Vesuvius volcano by means GPS measurements from 2001 to 2012. In this study we use a dataset from nine continuous GPS stations of the Neapolitan Volcanoes Continuous GPS network (NeVoCGPS), which covers the Neapolitan volcanic area, and is operated by the Istituto Nazionale di Geofisica e Vulcanologia. The GPS data processing is performed by the Bernese software v. 5.0. The results of the data processing show that the dynamics of the Somma-Vesuvio volcano, between 2001 and 2012, is characterized by a general subsidence, with maximum values on the Gran Cono at BKNO (−11.7 ± 0.65 mm/year) and BKE1 (−4.92 ± 0.36 mm/year) stations. The subsidence decrease from the crater down to the coast and the horizontal displacements are concentrated in Gran Cono area, the youngest part of the volcano. The parameters of the principal strain components indicate that Somma-Vesuvius is affected by a predominant contraction phase, which is concentrated in the areas with the greatest altitudes.

1. Introduction

The Somma-Vesuvius is a strato-volcano located 15 km east of Naples (Figure 1). It is about 1,200 meters high and covers a surface area of 165 km^2 [Principe et al. 1987]. About 2 million people live in the surroundings of the volcano: hence the Somma-Vesuvius may be considered a relatively small volcano with an associated high level of risk [Auger et al. 2001]. This is the main reason to demand for the improvement in knowledge regarding volcano structures and dynamics in recent years [e.g. Zollo et al. 1996a, 1996b, 1998, Bruno and Rapolla 1999, Cubellis et al. 2001, Del Pezzo et al. 2006, Berrino and Camacho 2008]. In particular, TOMOVES [Gasparini et al. 1998] and BROADVES [De Gori et al. 2001] projects have given a strong stimulus towards structural studies, considerably changing our ideas about the internal structure of volcano [De Natale et al. 2006]. In summary, the results of TOMOVES project has shown the following evidences: a) a high-velocity zone which extends vertically from about 400 m below the crater down to at least 3000 m and a shallow 300-500 m thick low-velocity layer which covers the edifice [Zollo et al. 1996a, 1996b]; b) a detailed image of the top of Mesozoic carbonate rocks forming the basement of the volcanic area. [Zollo et al. 2002]; c) an extended low-velocity layer at about 8-kilometer depth, interpreted as a sill with magma interspersed in a solid matrix [Auger et al. 2001, Capuano et al. 2003]. Moreover, the seismic tomography at a regional scale (BROADVES project) also put in evidence a low velocity anomaly under Somma Vesuvius volcano, between 15 and 35 km of depth [De Gori et al. 2001, De Natale et al. 2006].

Since the last eruption in 1944, the Somma-Vesuvius system has been in a quiescent phase. Its current activity is characterized by hundreds of earthquakes per year with low energy, low temperature fumaroles at the summit crater and subsidence. The largest earthquake (MD = 3.6) was recorded on October 1999 [Del Pezzo et al. 2004, De Natale et al. 2004, Galluzzo et al. 2004, Cubellis et al. 2007].

De Natale et al. [2000] have interpreted the seismicity in this quiescent period as mainly due to the gravitational loading of the volcanic edifice, coupled to a particular substructure in which central conduits, filled by quenched magma, are characterized by a marked rigidity contrast, focusing gravitational and any local and regional stresses. The gravitational loading (not only on the volcano) has been postulated by many authors [Prandtl 1921, Hencky 1923, Terada 1929, Borgia et al. 1992, Mc Guire et al. 1997], including flank instability and volcano spreading [Borgia et al. 2000a, 2000b, Lanari et al. 2002, Borgia et al. 2005, Guglielmino et al. 2011].

In this paper, we evaluate ground deformations at Somma-Vesuvius volcano, from 2001 until 2012, by

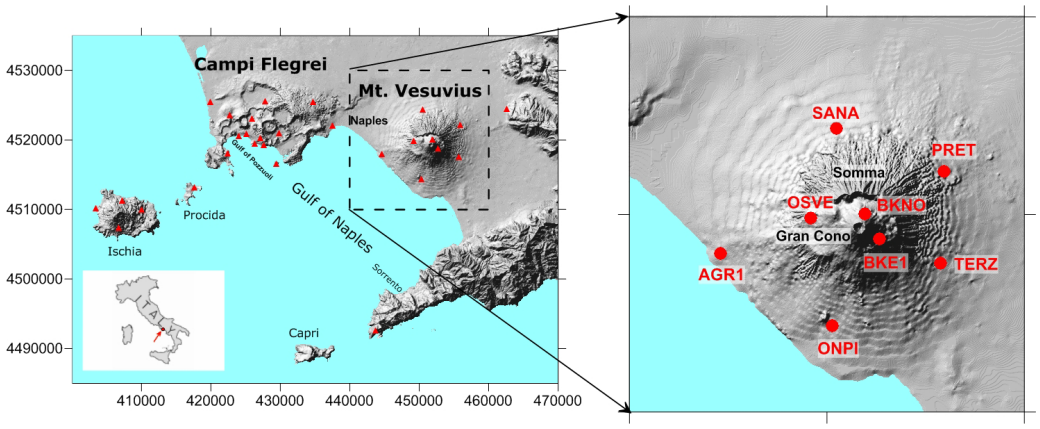

Figure 1. NeVoCGPS network. Red triangles indicate GPS stations of the network. In the insert box, the nine stations used in this study are shown.

using GPS data. From a ground deformation viewpoint, we show that the dynamics of volcano is characterized by diffuse subsidence and by planimetric movements concentrated only in the high elevation zone of Somma-Vesuvius.

2. Somma-Vesuvius GPS network and collected data

The first discontinuous GPS measurements at Somma-Vesuvius were carried out in 1992 [Pingue et al. 1998], but continuous observations began only four years later. Indeed, the first permanent GPS station was installed at Somma-Vesuvius in February 1996 and it recorded GPS data just for one week [Esposito et al. 2001]. However, only since 2001 the CGPS network had a stable configuration and all stations have been equipped with choke ring antennas (TERZ since 2003). Today, the Somma-Vesuvio GPS network is a part of a continuous GPS network (Figure 1), called NeVoCGPS (Neapolitan Volcanoes Continuous GPS) aimed monitoring of the entire Neapolitan volcanic area. It consists of 29 permanent stations equipped with dual-frequency receivers and choke ring antennas. Every day, 24 hours of observed dual-frequency GPS data, with 30 seconds sampling interval and 15 degrees cut-off angle, are downloaded from each site to the Osservatorio Vesuviano (Istituto Nazionale di Geofisica e Vulcanologia, Naples section), by the Internet, Wi-Fi and commercial telephone lines, depending on the communications infrastructure available at each station.

The data quality must be quickly and accurately tested before processing and storage in a database. The Osservatorio Vesuviano uses an in-house automatic application (SETA) for a quality check. It makes use of freeware programs, e.g. TEQC software [Estey and Meertens 1999], to translate from the binary receiver format to the standard RINEX format, perform a quality check of the data and zip the data files in an archive. All the procedures for managing the remote stations, downloading raw data, creating RINEX files and data quality control take place automatically.

In this study, we use continuous GPS measurements from nine sites of the NeVoCGPS network. The oldest stations (ONPI, PRET, and SANA) have been active for eleven years and the newest (BKNO) for 16 months. Table 1 shows the time span of the data sets and the equipment used in each station.

Site	Receiver + Antenna	Year of first observation	Time span interval (years)	Number of observations (weeks)	a.s.l. (m)
AGR1	Leica RS500 + LEIAT504 LEIS	2003	9	381	116
BKE1	Leica GRX1200PRO + LEIAT504 LEIS	2006	6	237	900
BKNO	Leica GRX1200GGPRO + LEIAT504GG LEIS	2010	2	72	1000
ENAV	Leica RS500 + LEIAT504 LEIS	2004	8	352	400
ONPI	Leica RS500 + LEIAT504 LEIS	2001	11	482	178
OSVE	Leica GRX1200Pro + LEIAT504 LEIS	2005	7	282	608
PRET	Leica RS500 + LEIAT504 LEIS	2001	11	442	256
SANA	Leica RS500 + LEIAT504 LEIS	2001	11	480	203
TERZ	Leica RS500 + LEIAT504 LEIS	2003	9	390	227

Table 1. Characteristics of the CGPS stations used in this paper and of the collected data. Station TERZ was equipped with choke ring antenna in 2003 and due radiofrequency interference first observation of OSVE started in 2005.

3. GPS data processing and time series

Data processing is performed by the Bernese Processing Engine (BPE) of the Bernese GPS software v. 5.0 [Dach et al. 2007] in double difference mode. The elevation cut off is set at 15° and the IGS absolute phase center variations (APCVs) for the satellite and receiver antennas are applied. The data are automatically processed on a daily basis using the Ultra-rapid International GNSS Service (IGS) products [Dow et al. 2009]. When the IGS final orbits and Earth orientation parameters (EOPs) become available, the data are reprocessed on a weekly basis.

Independent baselines are selected taking into account the criterion of maximum common observations [Dach et al. 2007]. The ambiguity resolution is based on the Quasi Ionosphere Free (QIF) analysis. Daily coordinates of the stations are estimated, together with the troposphere, in the final ionosphere free L3 solution. The dry part of the troposphere is modeled using the dry-Niell *a-priori* model and estimating the troposphere zenith delay (TZD) parameters every hour at each site using the wet-Niell mapping function. The geodetic datum is realized by three no-net-translation conditions imposed on a set of six IGS08 reference stations (minimum constraint solution), which are included in the processing. Table 2 shows the difference between the

Station	North (mm)	East (mm)	Up (mm)
CAGL 12725M003	0.4	2.9	-2.9
GRAS 10002M006	3.5	3.6	0.6
MATE 12734M008	2.4	-3.4	0.5
NOT1 12717M004	0.0	-3.1	-0.2
WTZR 14201M010	-1.9	2.0	0.4
ZIMM 14001M004	-2.1	-1.6	1.9
RMS / Component	2.3	3.1	1.6
RMS of Helmert transformation	2.3 mm		

Table 2. Residuals from Helmert transformation between IGS08 and solution for the reference stations.

SITE	Component	Velocity (mm/yr)	Flicker noise (mm/yr$^{1/4}$)	White noise (mm)
AGR1	North	0.21 ± 0.07	1.06 ± 0.14	0.57 ± 0.04
	East	0.37 ± 0.09	1.38 ± 0.14	0.53 ± 0.05
	Up	-0.28 ± 0.24	3.81 ± 0.39	1.17 ± 0.16
BKE1	North	-0.16 ± 0.13	1.30 ± 0.23	0.72 ± 0.07
	East	-1.67 ± 0.14	1.34 ± 0.28	0.87 ± 0.08
	Up	-4.92 ± 0.36	3.76 ± 0.53	1.55 ± 0.18
BKNO	North	-4.68 ± 0.23	----------	0.83 ± 0.07
	East	-2.32 ± 0.28	----------	1.04 ± 0.09
	Up	-11.71 ± 0.65	----------	2.41 ± 0.20
ONPI	North	0.28 ± 0.06	1.23 ± 0.19	0.69 ± 0.05
	East	0.10 ± 0.06	1.19 ± 0.12	0.57 ± 0.04
	Up	-1.70 ± 0.17	3.52 ± 0.35	1.53 ± 0.12
OSVE	North	-0.73 ± 0.11	1.21 ± 0.17	0.71 ± 0.05
	East	0.75 ± 0.10	1.20 ± 0.17	0.56 ± 0.05
	Up	-1.53 ± 0.27	3.12 ± 0.37	1.33 ± 0.13
PRET	North	0.06 ± 0.07	1.51 ± 0.16	0.60 ± 0.06
	East	-0.67 ± 0.08	1.51 ± 0.18	0.75 ± 0.06
	Up	-1.14 ± 0.20	3.90 ± 0.46	1.78 ± 0.16
SANA	North	-0.26 ± 0.07	1.46 ± 0.14	0.58 ± 0.05
	East	0.08 ± 0.07	1.33 ± 0.13	0.54 ± 0.05
	Up	-0.81 ± 0.19	3.96 ± 0.36	1.24 ± 0.15
TERZ	North	-0.12 ± 0.17	2.92 ± 0.11	0.00 ± 0.00
	East	-0.21 ± 0.14	2.38 ± 0.19	0.07 ± 0.63
	Up	-4.16 ± 0.60	10.20 ± 1.01	2.06 ± 0.56

Table 3. Results of the time series analysis for Somma-Vesuvio GPS permanent stations. The analysis and noise characterization are performed with CATS software [Williams 2008]. Due to the short time series (only 1.5 years), the flicker noise for BKNO station is not calculated.

IGS08 coordinates and estimated value for reference stations. Residuals demonstrate the consistency of estimated coordinates with IGS08 at level of 2.3 mm in total RMS from Helmert transformation. Velocity differences are very small (below 0.5 mm/yr) for all stations.

Daily and weekly GPS time series of the north, east and up components are calculated in the global IGS08 reference frame. The Neapolitan volcanic area is a part of the Eurasia plate, which has, in terms of GPS horizontal component, a velocity about 2.5 mm/yr to the NE. Therefore, to eliminate the global tectonic motion and highlight the volcanic deformation, the planimetric velocities of GPS permanent stations are calculated with respect to a local reference station (ENAV; Figure 1) located on the limestones of Sorrento Peninsula, outside the volcanic area, and with long time span of measurements and constant horizontal velocities. We subtract ENAV velocity (16.5 mm/yr and 21.3 mm/yr, in the north and east component respectively) from the GPS planimetric time series for every station [De Martino et al. 2011].

Afterwards, the time series are analyzed to determine noise properties, linear velocities and periodic signals using Maximum Likelihood Estimation (MLE). This technique allows simultaneous estimations of the noise properties structure together with the parameters of a time-dependent model of the data. The quantities estimated by MLE analysis are linear trend, offsets, annual and semi-annual periodic signals [Williams 2003]. The MLE analysis is performed using the CATS software

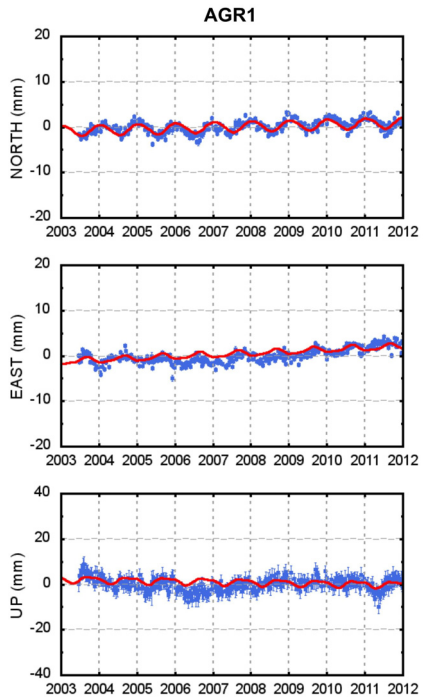

Figure 2. Weekly position time series of AGR1 GPS station. North and east components are relative to ENAV station. Red line represents the sum of linear trend, annual and semi-annual periodic signals estimated with the CATS software.

[Williams 2008], and all the parameters are estimated with white plus flicker error models [Langbein and Johnson 1997, Mao et al. 1999, Williams 2003, Amiri-Simkooei et al. 2007]. Their uncertainties can thus be considered to be realistic estimates based on the analysis of the noise at each station [Avallone et al. 2010]. The analysis results are listed in Table 3 and shown in Figure 2.

Ground deformations can be considered as the superposition of a background signal, which is equal at all GPS stations, plus a local signal. For background deformation we intend a stationary level of deformation in which every transient can be considered indicative of changes in the studied area.

A time-series is stationary at the *n*th order if its statistical moment of order *n* is time independent. In our case, a deformation transient can easily be recognized because it significantly perturbs the average value of a stationary signal [Bottiglieri et al. 2007].

The stationarity has been tested using a two-tailed *t*-test at significance level *t* 95% for constant length running windows: the mean in each time window has been evaluated and then all the possible couples of means have been compared to another. A signal is considered stationary when the 98% of the averages can be considered equal to a 95% significance level [Bottiglieri et al. 2007].

As a result we find that the UP components exhibiting a deformation trend are those from the stations BKE1, BKNO, ONPI, OSVE, PRET, SANA, and TERZ stations. Instead, regarding horizontal components, only the stations located in the maximum vertical displacements area (BKNO, BKE1, OSVE) and PRET station on Mt. Somma show significant planimetric movements.

4. Discussion and conclusion

The GPS data presented in this paper show that the dynamics of the Somma-Vesuvio volcano, between 2001 and 2012, is characterized by a general subsidence (Table 3), with maximum values on the Gran Cono (BKNO -11.7 ± 0.65 mm/year and BKE1 -4.92 ± 0.36 mm/year). Down to the volcano foot, from Gran Cono to Mt. Somma, the subsidence velocity decreases until reaching the minimum values on the coast, where the station at a lowest altitude (AGR1) has a velocity (-0.28 ± 0.24 mm/year) comparable to the error. This is confirmed by data from the tide gauge network [Tammaro et al. 2007, Obrizzo et al. 2009] and from the leveling network [Pingue et al. 2013]. Comparison between the velocity of the leveling benchmarks close to GPS stations and UP velocity of GPS sites is shown in Figure 5 and Table 4.

It is evident from Figure 3, which shows altitude of GPS stations *versus* subsidence velocity, and from Figure 4, which show the load (ρ*g*h) with respect to

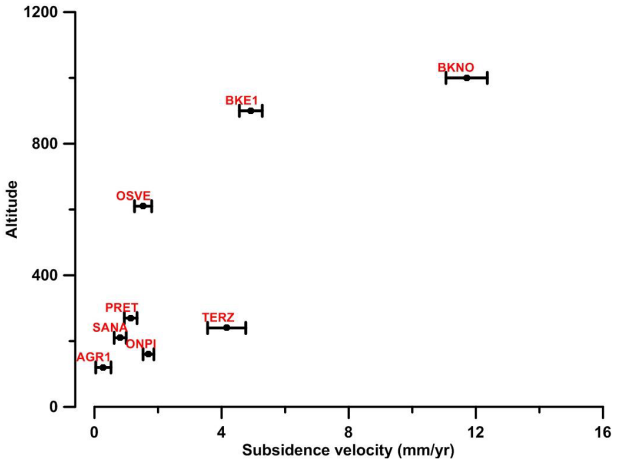

Figure 3. Altitude of GPS stations *versus* subsidence velocity.

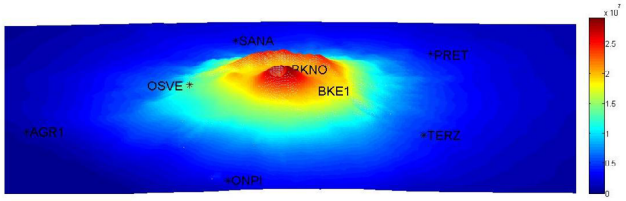

Figure 4. Gravitational load (ρ*g*h) as function of the volcano topography.

the volcano topography, that the GPS stations with highest velocities are those located at higher altitudes, on the Gran Cono. This is to be expected, since the stations at higher altitude are those with higher potential energy, and show that the vertical movements are also affected by the topography [Meo et al. 2008].

Lanari et al. [2002], from SAR and leveling data (1992-2000), show that the Somma-Vesuvius volcano is subject to a deformation process characterized by a continuous subsidence in the Vesuvius area (Gran Cono). However, this analysis is restricted to the vertical component and only in subsectors where the coherence of the interferometric signal is preserved (Gran Cono area) or, at lower altitudes, that are not covered by vegetation. On Somma-Vesuvius volcano, the terrestrial geodetic networks, such as leveling and GPS (NeVoCGPS) networks, cover areas that are not measured by the SAR.

If we consider the altitude *versus* modulus of horizontal velocity (Figure 6), we note that as the altitude

GPS station	UP velocity (mm/year)	Leveling benchmark	Velocity (mm/year)
BKE1	-4.92 ± 0.36	LVE/019	-5.00 ± 0.35
BKNO	-11.71 ± 0.65	LVE/013	-7.95 ± 0.37
ONPI	-1.7 ± 0.17	LVE/051N	-1.35 ± 0.29
OSVE	-1.53 ± 0.27	LVE/085	-1.52 ± 0.34

Table 4. GPS velocities and average velocity of the leveling benchmarks closest to GPS station.

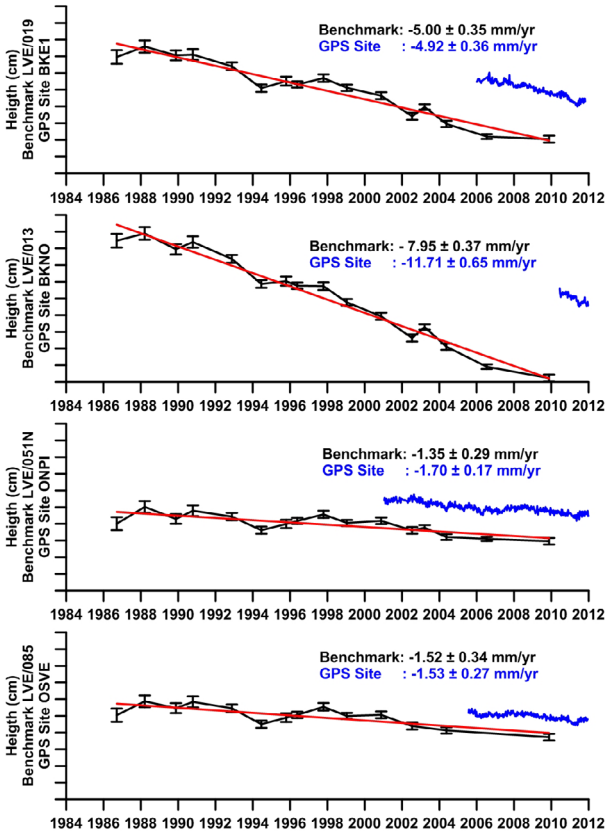

Figure 5. Time series of leveling benchmarks closest to GPS stations and comparison between benchmark and GPS velocities. Red line show linear fit of leveling data. The offset between each couple of time series is arbitrary. The Y scale is linear and spacing tick is of 2 cm.

increases, planimetric velocity increases. Horizontal velocity below 300 meters is less than 1 mm/yr, only the GPS stations above 600 m (Gran Cono area) have velocity > 1 mm/yr.

The horizontal velocities of the GPS stations located at Mt. Somma (Figure 7) seem unaffected by the presence of the volcano. Indeed, the values of horizontal velocities are comparable to the error and vary from (0.24 ± 0.22) mm/yr to (0.37 ± 0.26) mm/yr, except PRET, which has a velocity of (−0.67 ± 0.08) mm/yr.

We have calculated the parameters of the principal strain components starting from displacements evaluated in the longer period of time (over 10 years) estimated by the velocity of the seven permanent GPS stations and considered constant for the whole period. Only BKNO station is not considered, due to its too short operating time (about 1.5 years). The main strain parameters refer to the barycenters of the seven triangles in which the area covered by the GPS stations was divided. The results obtained (Figure 8) indicate, as already in the past [Bonasia and Pingue 1981] that Somma-Vesuvius is affected by a predominant contraction phase, albeit small (less than 10 ppm). This contraction phase is more marked (Figure 8) in the areas with the greatest altitudes, according to the phenomenon of diffuse and modest subsidence observed in the Gran Cono area [Bonasia and Pingue 1981,

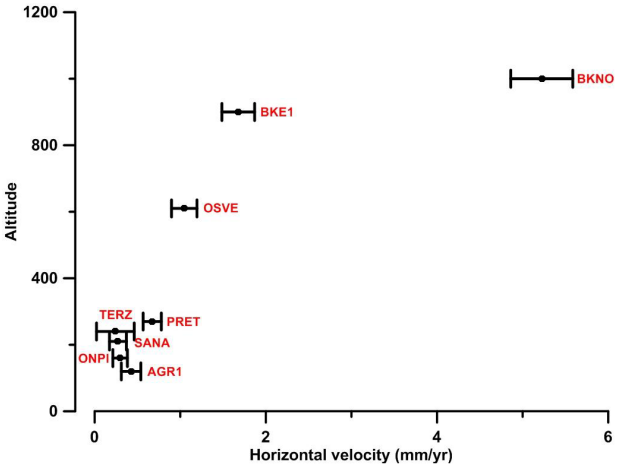

Figure 6. Altitude of GPS stations *versus* horizontal velocity.

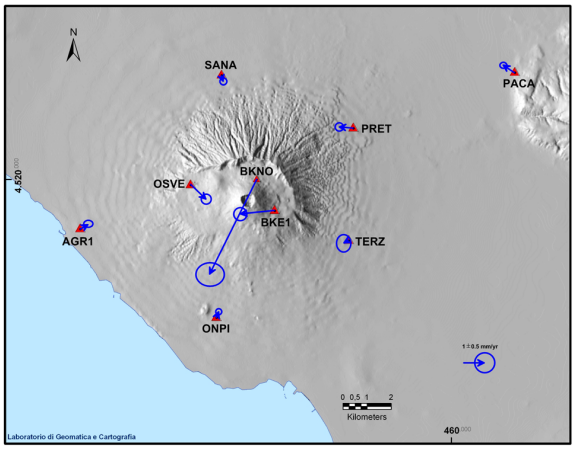

Figure 7. The horizontal GPS velocity field (relative to ENAV) and the 95 per cent confidence ellipse.

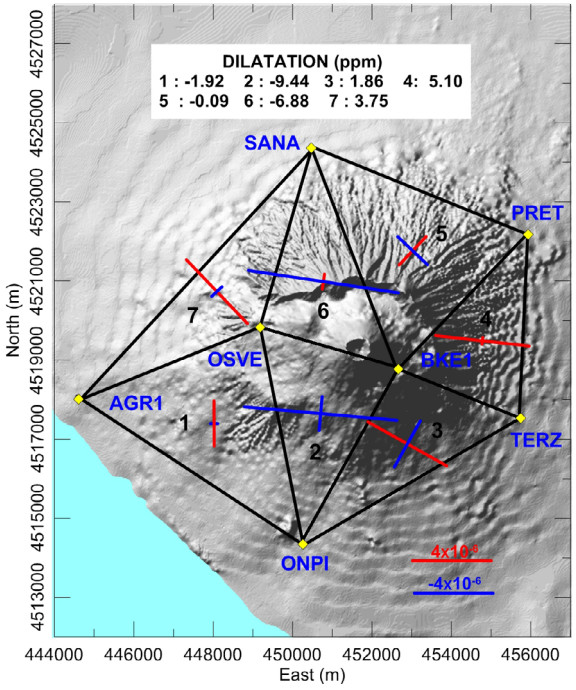

Figure 8. Principal strain axes for each of the seven triangles in which Vesuvius area has been divided. In the insert the dilatation values (in ppm) are also shown.

Pingue and Esposito 1988, Pingue et al. 1998, Lanari et al. 2002, Pingue et al. 2013].

We argue that a key to understanding the static deformation in Gran Cono area is the joint effect of compaction, sliding, including flank instability, and gravitational stress. As already suggested by Lanari et al. [2002], the discontinuity between the younger Vesuvius and the older Mt. Somma structure is not so well defined, but it is likely inward dipping with a normal fault-like sliding. This occurrence is also favored by the regional extensional tectonic regime in the area [Montone 1995]. Subsidence around the Gran Cono also is in agreement with the hypothesis that local seismicity, clustered below the crater itself, is mainly driven by gravitational stress [De Natale et al. 2000, 2006, D'Auria et al. 2013].

Instead, static deformation (mainly subsidence) at Mt. Somma area is due to the contact, at a greater depth, between volcanic edifice and the sedimentary sequence below the volcano. It may also be induced by normal fault-like slip with a low angle dip, occurring along the contact zones between the volcanic rocks and the carbonatic basement due to the joint effect of the tensional regional stress regime and the volcano loading [Lanari et al. 2002, De Natale et al. 2006].

Acknowledgements. The authors are indebted to the reviewers, because without their useful comments and suggestions, the manuscript could not have been completed in its present form. The authors express their gratitude to Mario La Rocca, Associate editor of Annals of Geophyisics.

References

Amiri-Simkooei, A.R., C.C.J.M. Tiberius, P.J.G. Teunissen (2007). Assessment of noise in GPS coordinate time series: methodology and results, J. Geophys. Res., 112, B07413; doi:10.1029/2006JB004913.

Auger, E., P. Gasparini, J. Virieux and A. Zollo (2001). Seismic evidence of an extended magmatic sill under Mt. Vesuvius, Science, 294, 1510-1512.

Avallone, A., G. Selvaggi, E. D'Anastasio, N. D'Agostino, G. Pietrantonio, F. Riguzzi, E. Serpelloni, M. Anzidei, G. Casula, G. Cecere, C. D'Ambrosio, P. De Martino, R. Devoti, L. Falco, M. Mattia, M. Rossi, F. Obrizzo, U. Tammaro and L. Zarrilli (2010). The RING network: improvement of a GPS velocity field in the Central Mediterranean, Annals of Geophysics, 53 (2), 39-54; doi: 10.4401/ag-4549. ISSN:1593-5213.

Berrino, G., and A.G. Camacho (2008). 3D Gravity Inversion by Growing Bodies and Shaping Layers at Mt. Vesuvius (Southern Italy), Pure Appl. Geophys., 165, 1095-1115; doi:10.1007/s00024-008-0348-2.

Bonasia, V., and F. Pingue (1981). Ground Deformations on Mt. Vesuvius from 1977 to 1981, Bull. Volcanol., 44 (3), 513-520.

Borgia, A., L. Ferrari and G. Pasquarè (1992). Importance of gravitational spreading in the tectonic and volcanic evolution of Mount Etna, Nature, *357*, 231-235.

Borgia, A., P.T. Delaney and R.P. Denlinger (2000a). Spreading volcanoes, Annu. Rev. Earth Planet. Sci. *28*, 539-570.

Borgia, A., R. Lanari, E. Sansosti, M. Tesauro, P. Berardino, G. Fornaro, M. Neri and J.B. Murray (2000b). Actively growing anticlines beneath Catania from the distal motion of Mount Etna's decollement measured by SAR interferometry and GPS, Geophys. Res. Lett., *27*, 3409-3412.

Borgia, A., P. Tizzani, G. Solaro, M. Manzo, F. Casu, G. Luongo, A. Pepe, P. Berardino, G. Fornaro, E. Sansosti, G.P. Ricciardi, N. Fusi, G. Di Donna and R. Lanari (2005). Volcanic spreading of Vesuvius, a new paradigm for interpreting its volcanic activity, Geophys. Res. Lett., *32*, L03303; doi:10.1029/2004GL 022155.

Bottiglieri, M., M. Falanga, U. Tammaro, F. Obrizzo, P. De Martino, C. Godano and F. Pingue (2007). Independent component analysis as a tool for ground deformation analysis, Geophys. J. Int., 168, 1305-1310; doi:10.1111/j.1365-246X.2006.03264.x. ISSN:0956-540X.

Bruno, P.P.G., and A. Rapolla (1999). Study of the subsurface structure of Somma-Vesuvius (Italy) by seismic reflection data, J. Volcanol. Geoth. Res., *92* (3-4), 373-387.

Capuano, P., P. Gasparini, A. Zollo, J. Virieux, R. Casale and M. Yeroyanni, eds. (2003). The Internal Structure of Mt. Vesuvius: a seismic tomography investigation. Napoli, Liguori editore, 595 pp.

Cubellis, E., M. Ferri, G. Luongo and F. Obrizzo (2001). The roots of Mt. Vesuvius from gravity anomalies, Mineralogy and Petrology, *73*, 23-38.

Cubellis, E., G. Luongo and A. Marturano (2007). Seismic hazard assessment at Mt. Vesuvius: the maximum magnitude expected, J. Volcanol. Geoth. Res., 162, 139-149; doi:10.1016/j.jvolgeores.2007.03.003.

Dach, R., U. Hugentobler, P. Fridez and M. Meindl (2007). Bernese GPS Software version 5.0, Astronomical Institute, Univ. of Bern, Bern, Switzerland.

D'Auria, L., A.M. Esposito, D. Lo Bascio, P. Ricciolino, F. Giudicepietro, M. Martini, T. Caputo, W. De Cesare, M. Orazi, R. Peluso, G. Scarpato, C. Buonocunto, M. Capello and A. Caputo (2013). The recent seismicity of Mt. Vesuvius: inference on seismogenic processes, Annals of Geophysics, *56* (4), S0442; doi:10.4401/ag-6448.

De Gori, P., G.B. Cimini, C. Chiarabba, G. De Natale, C. Troise and A. Deschamps (2001). Teleseismic tomography of the Campanian volcanic area and surrounding Apenninic belt, J. Volcanol. Geoth. Res., 109 (1-3), 52-75.

Del Pezzo, E., F. Bianco and G. Saccorotti (2004). Seismic Source Dynamics at Vesuvius Volcano, Italy. J. Volcanol. Geoth. Res., 133 (1-4), 23-39.

Del Pezzo, E., F. Bianco, L. De Siena and A. Zollo (2006). Small scale shallow attenuation structure at Mt. Vesuvius, Italy, Physics of the Earth and Planetary Interiors, 157, 257-268.

De Martino, P., U. Tammaro, F. Obrizzo, V. Sepe, G. Brandi, A. D'Alessandro, M. Dolce and F. Pingue (2011). La rete GPS dell'isola d'Ischia: deformazioni del suolo in un'area vulcanica attiva (1998-2010), Quaderni di Geofisica, INGV, no. *95*, 59 pp. ISSN:1590-2595.

De Natale, G., S.M. Petrazzuoli, C. Troise, F. Pingue and P. Capuano (2000). Internal stress field at Mt. Vesuvius: a model for the generation of background seismicity at a central volcano, J. Geophys. Res., 105 (B7), 16207-16214.

De Natale, G., C. Troise, R. Trigila, D. Dolfi and C. Chiarabba (2004). Seismicity and 3D substructure at Somma-Vesuvius volcano: evidence for magma quenching, Earth Plan. Sci. Lett., 221, 181-196.

De Natale, G., C. Troise, F. Pingue, G. Mastrolorenzo and L. Pappalardo (2006).The Somma-Vesuvius volcano (Southern Italy): Structure, dynamics and hazard evaluation, Earth-Science Reviews, 74, 73-111.

Dow, J.M., R.E. Neilan and C. Rizos (2009). The International GNSS Service in a changing landscape of Global Navigation Satellite Systems, Journal of Geodesy, 83, 191-198; doi:10.1007/s00190-008-0300-3.

Esposito, T., V. Grassi, S. Malaspina, C. Serio and U. Tammaro (2001). Rilevamento dei movimenti del suolo al Somma-Vesuvio. Criteri di progettazione e prospettive di sviluppo delle reti esistenti, Bollettino SIFET, *3*, 31-46.

Estey, L., and C. Meertens (1999). TEQC: The Multi-Purpose Toolkit for GPS/GLONASS Data, GPS Solutions, *3* (1), 42-49.

Galluzzo, D., E. Del Pezzo, M. La Rocca and S. Petrosino (2004). Peak Ground Acceleration produced by local earthquakes in volcanic areas of Campi Flegrei and Mt. Vesuvius, Annals of Geophysics, 47 (4), 1377-1390.

Gasparini, P., and Tomoves Working Group (1998). Looking inside Mt. Vesuvius, EOS Trans. AGU, 79 (229, 230, 232).

Guglielmino, F., C. Bignami, A. Bonforte, P. Briole, F. Obrizzo, G. Puglisi, S. Stramondo and U. Wegmuller (2011). Analysis of satellite and *in situ* ground deformation data integrated by the SISTEM approach: the April 3, 2010 earthquake along the Pernicana fault (Mt. Etna – Italy), EEPSL, 312, 327-336.

Hencky, H. (1923). Über einige statisch bestimmte Fälle des Gleichgewichts in plastischen Körpern, Zeitscrift für angewandte mathematic und mechanic, *3* (4), 241-251.

Lanari, R., G. De Natale, P. Berardino, E. Sansosti, G.P. Ricciardi, S. Borgstrom, P. Capuano, F. Pingue and C. Troise (2002). Evidence for a peculiar style of ground deformation inferred at Vesuvius volcano, Geophys. Res. Lett., *29* (9), 1292; doi:10.1029/2001 GL014571.

Langbein, J., and H. Johnson (1997). Correlated error in geodetic time series: Implications for time-dependent deformation, J. Geophys. Res., 102 (B1), 591-604.

Mao, A., C.G.A. Harrison and T.H. Dixon (1999). Noise in GPS coordinate time series, J. Geophys. Res., 104, 2797-2816.

Mc Guire, W. J., I.S. Stewart and S. J. Saunders (1997). Intra-volcanic rifting at Mount Etna in the context of Regional tectonics, Acta Vulcanol., 9, 147-156.

Meo, M., U. Tammaro and P. Capuano (2008). Influence of topography on ground deformation at Mt. Vesuvius (Italy) by finite element, Int. J. Non-Lin. Mech., 43, 178-186.

Montone, P., C. Chiarabba and A. Amato (1995). State of stress in the Quaternary volcanoes from Tuscany to Campania, Per. Mineral., 64, 231-232.

Obrizzo, F., U. Tammaro, P. Capuano, F. Di Sena, A. La Rocca, S. Pinto, P. De Martino, E. Vertechi and F. Pingue (2009). Tide gauge network and vertical ground displacements in the Neapolitan volcanic area, In: Conferenza A. Rittmann "La vulcanologia italiana: stato dell'arte e prospettive future" (Nicolosi (Catania), Italy, June 11-13, 2009), 226-227. ISBN 978-88-89972-11-3.

Pingue, F., and T. Esposito (1988). Misure di livellazione di precisione nell'area vesuviana, Bollettino di Geodesia e Scienze Affini, 47 (3), 275-300.

Pingue, F., C. Troise, G. De Luca, G. Grassi and R. Scarpa (1998). Geodetic monitoring of Mt. Vesuvius Volcano, Italy, based on EDM and GPS surveys, J. Volcanol. Geoth. Res., 82, 151-160.

Pingue, F., M. Bottiglieri, C. Godano, F. Obrizzo, U. Tammaro, T. Esposito and C. Serio (2013). Spatial and temporal distribution of vertical ground movements at Mt. Vesuvius in the period 1973-2009, Annals of Geophysics, 56 (4), S0451; doi:10.4401/ag-6457.

Prandtl, L. (1921). Über die Eindringunsfestigkeit (Härte) plastischer Baustoffe und die Festigkeit von Schneiden, Zeitscrift für angewandte mathematic und mechanic, 1, 15-20.

Principe, C., M. Rosi, R. Santacroce and A. Sbrana (1987). Explanatory notes to the geological map, In: R. Santacroce (ed.), Somma-Vesuvius, Quaderni de "La Ricerca Scientifica", CNR, 114 (Progetto finalizzato Geodinamica, Monografie finali, 8), 11-52. ISSN: 0556-9664.

Tammaro, U., F. Di Sena, P. Capuano, F. Obrizzo, A. La Rocca, S. Pinto, A. Russo, P. De Martino and F. Pingue (2007). Deformazioni del suolo mediante analisi dei dati mareografici nell'area vulcanica napoletana nel periodo 1999-2006, Torino, ASITA, 2079-2084.

Terada, T. (1929). On the form of volcanoes, Bull. Earthquake Res. Inst., Univ. Tokyo, 7, 207-221.

Williams, S.D.P. (2003). The effect of coloured noise on the uncertainties of rates estimated from geodetic time series, Journal of Geodynamics, 76, 483-494.

Williams, S.D.P. (2008). CATS: GPS coordinate time series analysis software, GPS Solutions, 12 (2), 147-153; doi:10.1007/ s10291-007-0086-4.

Zollo, A., P. Gasparini, J. Virieux, H. Le Meur, G. De Natale, G. Biella, E. Boschi, P. Capuano, R. De Franco, P. Dell'Aversana, R. De Matteis, I. Guerra, G. Iannaccone, L. Mirabile and G. Vilardo (1996a). Seismic Evidence for a low velocity zone in the upper crust underneath Mt. Vesuvius, Science, 274 (5287), 592-594.

Zollo, A., P. Gasparini, G. Biella, R. de Franco, B. Buonocore, L. Mirabile, G. De Natale, G. Milano, F. Pingue, G. Vilardo, P.P. Bruno, R. De Matteis, H. Le Meur, G. Iannaccone, A. Deschamps, J. Virieux, A. Nardi, A. Frepoli, I. Hunstad and I. Guerra (1996b). 2D seismic tomography of Somma-Vesuvius: Description of the experiment and preliminary results, Annali di Geofisica, 39 (3), 471-486.

Zollo, A., P. Gasparini, J. Virieux, G. Biella, E. Boschi, P. Capuano, R. De Franco, P. Dell'Aversana, R. De Matteis, G. De Natale, G. Iannaccone, H. Le Meur and L. Mirabile (1998). An image of Mt. Vesuvius obtained by 2D seismic tomography, J. Volcanol. Geoth. Res., 82 (1-4), 161-173.

Zollo, A., L. D'Auria, R. De Matteis, A. Herrero, J. Virieux and P. Gasparini (2002). Bayesian estimation of 2-D P-velocity models from active seismic arrival time data: imaging of the shallow structure of Mt. Vesuvius (Southern Italy), Geophys. J. Int., 151, 566-582.

*Corresponding author: Umberto Tammaro,
Istituto Nazionale di Geofisica e Vulcanologia, Sezione di Napoli, Osservatorio Vesuviano, Naples, Italy;
email: umberto.tammaro@ov.ingv.it.